RESEARCH FRONT

CSIRO PUBLISHING

Aust. J. Chem. **2013**, *66*, 1048–1056
http://dx.doi.org/10.1071/CH13147

Full Paper

Electrochromic π-Conjugated Copolymers Derived from Azulene, Fluorene, and Dialkyloxybenzothiadiazole

Shaun Zhi Hao Lim,[A,B] *Wei Teng Neo,*[A] *Ching Mui Cho,*[A]
Xiaobai Wang,[A] *Angeline Yan Xuan Tan,*[A] *Hardy Sze On Chan,*[B]
and Jianwei Xu[A,C]

[A]Institute of Materials Research and Engineering, Agency for Science, Technology and Research (A*STAR), 3 Research Link, Singapore 11760.
[B]Department of Chemistry, National University of Singapore, 3 Science Drive 3, Singapore 117543.
[C]Corresponding author. Email: jw-xu@imre.a-star.edu.sg

A series of random π-conjugated copolymers **P1**, **P2**, and **P3** were synthesised from 1,3-dibromoazulene, 4,7-dibromo-5,6-bis(dodecyloxy)benzo-2,1,3-thiadiazole, and 9,9-dioctylfluorene-2,7-bis(trimethyleneborate) via Suzuki coupling reactions. The copolymers **P1–3** had molecular weights in the range of 17000–30900 g mol^{-1} with polydispersity indexes of 1.45–2.03. Thermal analysis showed that the polymers **P1–3** had good thermal stability with decomposition temperatures ranging from 341 – 363°C both in air and in nitrogen. Photoluminescence studies showed that polymer **P1** and **P2** are weakly fluorescent with low quantum yields of 0.013 and 0.0029 for **P1** borne with 30 % azulene and **P2** borne with 50 % azulene in the polymer backbone, respectively. **P3** borne with 70 % azulene resulted in complete quenching of fluorescence. The electrochemical band gaps for **P1**–**3** are very close to their corresponding optical band gaps. Electrochromic study showed that three polymer thin films displayed the same colour change from yellowish green at the neutral and electrochemically-reduced state to greyish brown at the electrochemically-oxidised state. In particular, electrochromic contrasts of 17 % and 13 % for **P2** and **P3**, respectively, were recorded in the near infrared region.

Manuscript received: 5 April 2013.
Manuscript accepted: 17 July 2013.

Introduction

Studies of organic conjugated polymers today have resulted in their electronic applications such as organic light-emitting diodes,[1] organic field-effect transistors,[2] organic photovoltaics,[3] as well as electrochromic devices.[4] The growing interest of organic conjugated polymers arises from the ability to fine-tune their properties through the modification of the conjugated polymer structures. This allows for the polymers to be tailored for their desired applications. Organic conjugated polymers also possess other advantages such as mechanical flexibility, low-cost, scalability, and processing.[5] Electrochromism can be defined as the reversible colour change induced by an external voltage.[4] Since this phenomena in the semiconductor tungsten oxide was first discovered by Deb in 1969,[6] most work has focussed on inorganic electrochromic materials such as the oxides of molybdenum (MoO_3) and titanium (TiO_2). Inorganic electrochromic materials are known to have high photochemical stability, however, they are costly to fabricate, exhibit slow response times and have low coloration efficiency.[4,7] Incorporation of conductive conjugated polymers in electrochromic devices offers many advantages, for example, they are easier to process and have faster response times and higher optical contrasts than inorganic electrochromic material-based devices.[4,8] These unique characteristics allow organic electrochromes to be potentially utilised in many applications such as non-emissive displays and smart windows.[5] However, the main shortcoming for electrochromic conjugated polymer materials is the redox stability. Some approaches have been attempted to solve this issue, such as the donor-acceptor (D-A) approach, which involves electron-rich donors and electron-poor acceptors within a polymer backbone. By controlling the composition of electron-rich and electron-poor moieties in the polymer chain, we can control HOMO and LUMO levels and ultimately the energy of the intraband transitions in D-A type conjugated polymers.

Currently, most electrochromic polymers are based on 3,4-alkylenedioxythiophene derivatives with neutral state colour spanning a full colour palette as well as transmissive oxidised states.[9] Structural modifications and particularly the D-A approach were utilised to design a variety of conjugated polymers. For example, fused heterocycle units containing high heteroatom content such as benzothiadiazole are commonly utilised as an electron acceptor. Due to the presence of electron-withdrawing nitrogen atoms within the heterocycle, benzothiadiazole derivatives are electron-deficient, acting as ideal electron acceptors. Many D-A type conjugated polymers containing benzothiadiazole derivatives have also been reported to show high hole mobility, low band gaps, as well as wide optical absorption bands[10] for organic field-effect transistor and organic photovoltaic applications. In this work, following a similar D-A approach, 5,6-dialkoxy-2,1,3-benzothiadiazole was adopted to design and synthesise azulene and fluorene-containing conjugated polymers. Azulene is a molecule consisting of two fused aromatic rings, namely, a seven-membered ring and a five-membered ring. Azulene and its derivatives are known to have interesting electronic properties such as low ionisation energy as well as a tendency to form radical cations and anions.[11] In addition, azulene has a relatively low oxidation potential (0.96 V vs saturated calomel electrode, SCE)[12] as compared with similar fused aromatics such as naphthalene, which has the same molecular formula (1.64 V vs SCE).[13] Thus, it is expected that azulene units in polymers are oxidised readily, which may result in interesting electrochromic properties. Poly(azulene)[14] and azulene-containing copolymers[15] including electrochromic conjugated copolymers, for example, poly(azulene-*alt*-fluorene), have been reported recently, however, they have shown low switching stability of several cycles as well as slow bleaching times.[15e] The introduction of 5,6-dialkyloxy-2,1,3-benzo[3,4]thiadiazole as an electron acceptor to the azulene-fluorene copolymers is hypothesised to improve the electrochromic properties of the polymers by lowering the band gap and avoiding over-oxidation of copolymers. Herein we report the synthesis and characterisation of a series of azulene-containing conjugated copolymers that are composed of varying ratios of electron donor and acceptor units.

Experimental

Materials

All reagents and chemicals, unless otherwise stated, were obtained from Aldrich, Alfa Aesar, or Lancaster and were used as received. Tetrahydrofuran was distilled over sodium/benzophenone. Triethylamine (TEA) was purified by refluxing with potassium hydride followed by distillation. 9,9-Dioctylfluorene-2,7-bis(trimethyleneborate) was recrystallised in hexane before use. Acetonitrile (ACN) was purchased from Baker, dried over Type 4Å 1–2 mm molecular sieve beads (International Laboratory USA) and filtered using 0.22 μm PVDF syringe filters (Millipore Millex-GV) before use. Indium tin oxide (ITO, 60 Ω/sq) coated poly(ethylene terephthalate) (PET) was obtained from Aldrich and used as the substrate.

Instrumentation

^{1}H NMR spectra were acquired on a 400 MHz DRX Bruker NMR spectrometer in $CDCl_3$ with TMS as the internal reference. The molecular weights of the polymers were determined on a Waters Model 2690 gel permeation chromatography (GPC) system using HPLC-grade THF at a flow rate of 1 mL min^{-1} and injection volume 10 μL with poly(methyl methacrylate) (PMMA) as standards. UV-Vis absorption spectra were measured using a Shimadzu UV-3101 spectrometer. The photoluminescence measurements were performed using a Perkin Elmer LS55 fluorescence spectrometer with a Xenon lamp as a light source, 10 nm Ex (excitation) and Em (emission) slits, 150 nm min^{-1} scan rate and 1 % attenuator. Thermal analysis was performed in a Perkin-Elmer thermogravimetric analyser (TGA 7) in nitrogen or in air at a heating rate of 10°C min^{-1} and a TA Instruments differential scanning calorimetry (DSC) 2920 at a heating rate and a cooling rate of 10°C min^{-1} in nitrogen. An Autolab PGSTAT128N potentiostat/galvanostat was used for cyclic voltammetry experiments and in situ spectro-electrochemical studies. A Shimadzu UV-3600 UV-Vis-NIRspectrophotometer was also employed for spectro-electrochemical studies. Photos were taken with a Canon Digital IXUS 50 digital camera.

Synthesis of Compounds **2**–**4**

1,2-Diamino-4,5-bis(dodecyloxy)benzene (**2**)

1,2-Bis(dodecyloxy)-4,5-dinitrobenzene (**1**) (1.0 mmol, 1 equiv.) and palladium on carbon (0.20 g, 10 wt-%) were added to a round-bottomed flask with 100 mL of ethanol. The mixture was stirred and purged under argon for ~1 h. Hydrazine monohydrate (2.0 mL, excess) was added dropwise to the suspension. The resultant reaction mixture was then heated up to reflux at 70°C until a colourless solution with black (carbon) suspension developed. The hot mixture was filtered using Celite and rinsed with hot ethanol. Excess solvent from the resulting filtrate was evaporated under reduced pressure to yield an off-white solid **2**, which was subsequently dried under vacuum for ~24 h. Compound **2** is easily oxidised in air, and it was used for the next reaction immediately after preparation. Yield: 96 %.

5,6-Bis(dodecyloxy)benzo-2,1,3-thiadiazole (**3**)

A Schlenk flask was first loaded with **2** (1.0 mmol, 1 equiv.) dissolved in a mixture of dry toluene (10 mL) and dry triethylamine (10 mL). The resultant mixture was degassed via five freeze-pump-thaw cycles under liquid nitrogen. After warming to room temperature, *N*-thionylaniline (0.30 mL, excess) was added to the stirring mixture. The resulting dark red solution was then left to stir for ~16 h before it was heated up to reflux at 120°C for ~3 h. Excess solvent was evaporated under reduced pressure and the resulting crude product was triturated with deionised water (40 mL). The crude product was filtered off and the residue was then recrystallised twice using hot ethanol to yield compound **3** as an off-white solid (0.315 g, 70 %). ^{1}H NMR ($CDCl_3$): δ 7.13 (s, 2H), 4.09 (t, 4H), 1.91 (m, 4H), 1.26 (m, 28H), 0.88 (t, 6H).

4,7-Dibromo-5,6-bis(dodecyloxy) benzo-2,1,3-thiadiazole (**4**)

To a dissolved mixture of **3** (1.0 mmol) in dichloromethane (16 mL) and acetic acid (7 mL), was added dropwise molecular bromine (6.0 mmol), and the resulting mixture was stirred in the dark for ~48 h at room temperature. The reaction mixture was then poured into a separatory funnel containing deionised water (20 mL). The desired product was extracted with dichloromethane followed by washing with water (40 mL), aqueous $NaHCO_3$ (40 mL) and aqueous Na_2SO_3 (40 mL). The organic layer obtained was dried over anhydrous $MgSO_4$ and excess solvent was evaporated under reduced pressure. The product was recrystallised with hot ethanol twice to obtain compound **4** as a fluffy off-white solid (0.455 g, 75 %). ^{1}H NMR ($CDCl_3$): δ 4.16 (t, 4H), 1.88 (m, 4H), 1.28 (m, 28H), 0.89 (t, 6H).

Synthesis of Polymers ***P1***–***3***

A Schlenk tube was first loaded with **4** (0.385 mmol), 9,9-dioctylfluorene-2,7-bis(trimethyleneborate) (0.550 mmol), and 1,3-dibromoazulene (0.165 mmol) dissolved in dry and degassed toluene (12 mL). A degassed aqueous solution (9.0 mL) of K_2CO_3 (2.50 g, 18.0 mmol), aliquat 336® (1 mL), and $Pd(PPh_3)_4$ (0.007 mmol) were added. The reaction mixture was purged under argon for ~30 min after which the reaction was run in a closed system at 105°C for 3 days. The reaction mixture was then poured into excess cold methanol (200 – 250 mL) with vigorous stirring. The obtained precipitate was filtered, washed with cold deionised water, and dried under vacuum. The crude product was dissolved in chloroform and filtered. The filtrate obtained was evaporated to dryness and dissolved in a minimal amount of toluene. The solution was added dropwise to a beaker of cold methanol (200 mL) with vigorous stirring to re-precipitate the polymer. The precipitate was then filtered and washed with acetone in a Sohxlet extractor for 2 days. The final product was obtained after drying in a vacuum oven for ~24 h as a greenish solid.

*Copolymer **P1***

Yield: 0.369 g, 91 %; ^{1}H NMR (CDCl$_3$): δ 8.63 – 8.65 (d, 0.6H), 8.33 (s, 0.3H), 7.70 – 7.96 (m, 6H), 7.16 (t, 0.6H), 3.94 (t, 2.8H), 2.10 – 2.17 (m, 4H), 1.57 (m, 6.8H), 1.28 – 1.38 (m 43.6H), 0.79 – 087 (d, 10.2H).

*Copolymer **P2***

Yield: 0.339 g, 83 %; ^{1}H NMR (CDCl$_3$): δ 8.56 – 8.58 (d, 1H), 8.26 (s, 0.5H), 7.63 – 7.88 (m, 6H), 7.09 (t, 1H), 3.87 (t, 2H), 2.03 – 2.10 (m, 4H), 1.48 – 1.55 (m, 8H), 1.15 – 1.20 (m, 38H), 0.78 – 0.86 (m, 9H).

*Copolymer **P3***

Yield: 0.377 g, 88 %; ^{1}H NMR (CDCl$_3$): δ 8.56 – 8.58 (d, 1.4H), 8.263 (s, 0.7H), 7.55 – 7.86 (m, 6H), 7.08 (t, 1.4H), 3.88 (t, 1.2H), 2.04 – 2.10 (m, 4H), 1.48 – 1.57 (m, 5.2H), 1.09 – 1.15 (m 32.4H), 0.72 – 0.86 (m, 7.8H).

Cyclic Voltammetry and Spectro-Electrochemistry

The solutions of polymers **P1–3** (10 mg mL^{-1} in *o*-xylene) were spin-coated onto ITO/PET using a SCS G3P-8 spincoater to form polymer thin films. For the cyclic voltammetry (CV) experiments, a three-electrode configuration was used with ITO coated PET as the working electrode, platinum wire (Metrohm) as the counter electrode and Ag/AgCl (3 M KCl) (Metrohm) as the reference electrode. A 0.1 M LiClO$_4$/ACN electrolyte/solvent couple was used. In situ spectro-electrochemical data was obtained using a three-electrode cell assembly, which consists of the ITO coated PET substrate as the working electrode, platinum wire as the counter electrode, and Ag wire as the pseudo-reference electrode.

Results and Discussion

Synthesis and Characterisation of Acceptor and Polymers

The synthetic route leading to polymers **P1–3** is outlined in Scheme 1. First, the reduction reaction of 1,2-dinitro-4,5-bis (dodecyloxy)benzene (**1**) was carried out in the presence of Pd/C and hydrazine to give a quantitative yield of 1,2-diamino-4,5-bis (dodecyloxy)benzene (**2**). Compound **2** underwent an intramolecular cyclisation reaction using *N*-thionylaniline according to the literature method with modification[16] to afford 5,6-bis (decyloxy)benzo-2,1,3- thiadiazole (**3**) in 70 % yield. In contrast to the reported method, the diamine **2** could be directly used in the cyclisation reaction instead of converting it into its diamino dihydrogen chloride. Compound **3** was brominated using molecular bromine to give 4,7-dibromo-5,6-bis(dodecyloxy) benzo-2,1,3-thiadiazole (**4**). Polymers **P1–3** were synthesised by reacting compound **4** and 1,3-dibromoazulene (**6**) with 9,9-dioctylfluorene-2,7-bis(trimethyleneborate) (**5**) via Suzuki coupling reaction in the presence of Pd(PPh$_3$)$_4$ catalyst (Scheme 1). The resultant crude copolymers were precipitated in methanol, followed by purification with Soxhlet extraction using acetone as solvent. Compositions, synthetic yields, molecular weights, polydispersity, and thermal data of the polymers **P1–3** are summarised in Table 1. **P1**, **P2**, and **P3** were obtained in good yield (91, 83, and 88 %, respectively). The polymers **P1–3** were structurally characterised by ^{1}H NMR and elemental analysis (Table S1 in the Supplementary Material), and their chemical structures and compositions are consistent with the expected structures. As an example, the ^{1}H NMR spectrum of the polymer **P2** is illustrated in Fig. 1. A doublet at δ 8.57 and a singlet at δ 8.26, corresponding to characteristic azulene protons H$_a$ and H$_b$, respectively, were observed. Azulene protons H$_c$ were overlapped with fluorene aromatic protons centred at δ 7.75. A triplet at δ 7.09 was assigned to azulene protons H$_d$. These suggested that azulene units were intact duration polymerisation. The distinctive signals at δ 2.03 from alkyl groups at the 9,9-position of the fluorene moiety and δ 3.87 from the alkoxy substituents of compound **4** were observed (Fig. 1). Polymers **P1** and **P3** showed similar NMR spectra profiles to the polymer **P1** and their spectra are given in the Supplementary Material (Fig. S1).

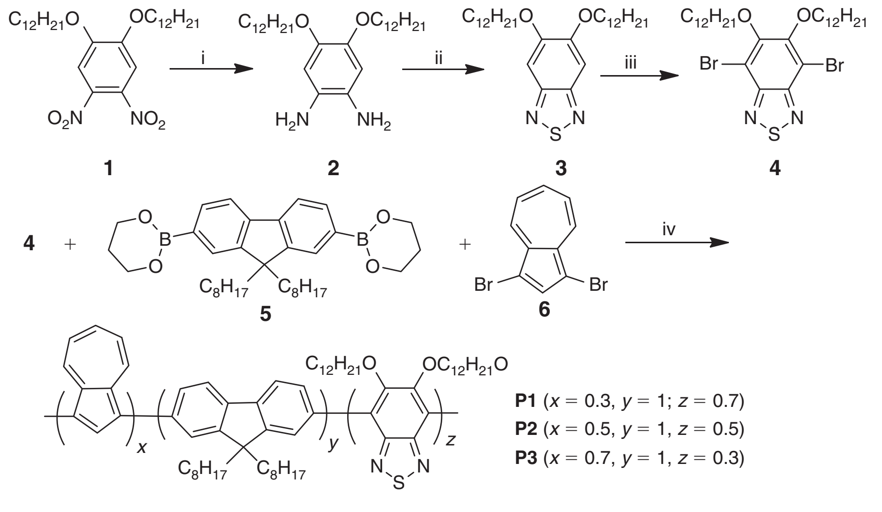

Scheme 1. Synthetic route leading to acceptor **4** and polymers **P1–3**. Reagents and conditions: (i) Hydrazine monohydrate, 10 % Pd/C, EtOH, argon, 70°C; (ii) *N*-thionylaniline, triethylamine (TEA), toluene, 120°C; (iii) bromine, acetic acid, dichloromethane, r.t.; (iv) toluene, aq. K$_2$CO$_3$, aliquat 336®, Pd(PPh$_3$)$_4$, 105°C, 3 d.

Table 1. Compositions, yields, molecular weights, polydispersity (M_w/M_n) and thermal data of polymers P1 – P3

M_w: the weight-average molecular weight; M_n: the number-average molecular weight; M_w/M_n: the polydispersity index

Polymer	Feed ratio x/y/z	Actual ratio x/y/z	Yield [%]	M_w	M_n	M_w/M_n	T_d In air	T_d In N_2
P1	0.30/1.00/0.70	0.30/0.99/0.72	91	62600	30900	2.03	360	350
P2	0.50/1.00/0.50	0.52/1.04/0.45	83	24600	17000	1.45	359	341
P3	0.70/1.00/0.30	0.71/1.02/0.27	88	41500	26400	1.57	363	356

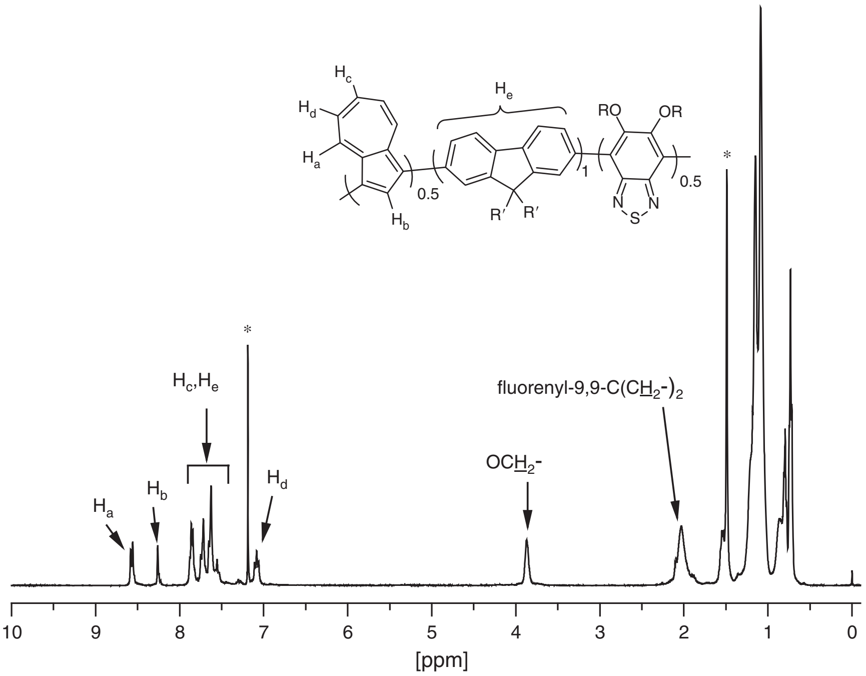

Fig. 1. ^{1}H NMR spectrum for polymer **P2**. *Residual solvents ($CHCl_3$ and H_2O).

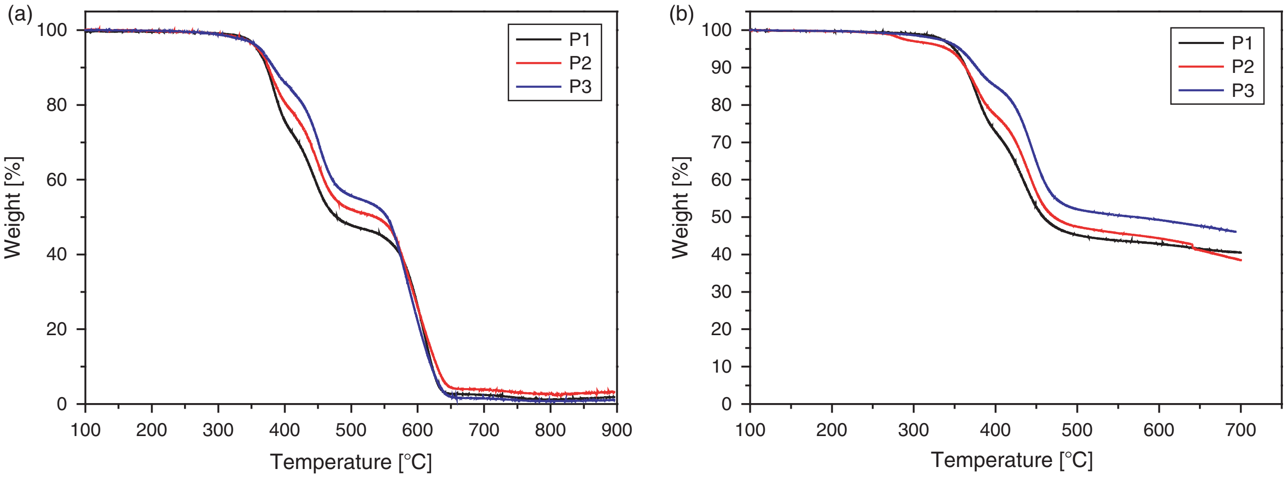

Fig. 2. Thermogravimetric graphs for polymers **P1–3** in (a) air and (b) nitrogen. The data was recorded at a rate of 10°C min^{-1}.

Polymer compositions were estimated by comparing the integration area of characteristic signals at δ 8.6, 3.9, and 2.1 of the three co-monomers **6**, **4**, and **5**, which are in good agreement with reactant feed ratios. Molecular weights of the polymers against poly(methyl methacrylate) standards were determined by GPC. All polymers had relatively high molecular weights ranging from 17000 – 30900 g mol^{-1} with reasonable polydispersity indexes (1.45–2.03). In addition, all polymers had good thermal stability with decomposition temperatures (T_d) in the range of 341 to 363°C in air and in nitrogen (Fig. 2). It was noteworthy that all polymers showed better thermal stability in inert atmosphere than in air. For example, the polymer **P1** has higher T_d by 10°C in air than in nitrogen. This may relate to the presence of the benzothiadiazole unit in the copolymer backbone. This monomer acts as anti-oxidant which may be oxidised to form benzo[2,1,3]thiadiazole 2,2-dioxide in air. The polymers were also studied by DSC and no glass transitions were detected.

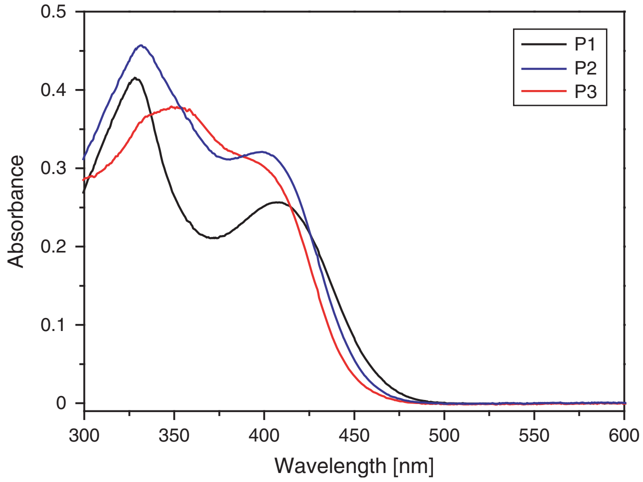

Fig. 3. UV-Vis absorbance spectra for **P1** (1.064×10^{-5} M), **P2** (1.239×10^{-5} M), and **P3** (1.339×10^{-5} M) in THF.

Table 2. Absorption λ_{max}, emission λ_{max}, optical band gap, and emission quantum yields of polymers P1 – P3

NA: not applicable

Polymer	Abs λ_{max} [nm]^A	abs λ_{onset} [nm]	E_g^{Opt} [eV]^B	Em λ_{max} [nm]	φ_{PL}
P1	328 (39000), 407 (24100)	520	2.38	509	0.013
P2	332 (36800), 399 (25900)	545	2.27	509	0.0029
P3	349 (28200), 392 (23200)	565	2.19	NA	NA

[A] The values in parentheses are molar absorptivities (ε) with units of L mol^{-1} cm^{-1}.

[B] Optical band gaps were calculated by the equation: $E_g^{Opt} = 1240/\text{abs}\ \lambda_{onset}$.

UV-Vis Spectroscopy and Photoluminescence Spectroscopy of Polymer Solution

The UV-Vis spectra and photoluminescence spectra of the polymers **P1–3**, together with the reference polymer poly (azluene-*alt*-dioctylfluorene) (**P4**) in THF solution were measured (Fig. 3). The UV-Vis absorption and photoluminescence data are summarised in Table 2. The reference polymer **P4** exhibited one strong π - π absorption band at 363 nm with molar absorptivity (ε) of 20500 L mol^{-1} cm^{-1}, a very weak shoulder peak at 477 (ε = 240 L mol^{-1} cm^{-1}), and a very weak broad band at 629 nm (ε = 190 L mol^{-1} cm^{-1}).[15e] In contrast, polymers **P1–3** showed two distinctive absorption peaks in the range of 328 to 349 nm (ε = 28200 – 39000 L mol^{-1} cm^{-1}) and between 392 and 407 nm (ε = 23200 – 24100 L mol^{-1} cm^{-1}). In contrast to reference polymer **P4**, no weak broad band was observed at long wavelengths. In comparison with the major absorption λ_{max} (363 nm) of the polymer **P4**, π-π absorption λ_{max} for the polymers **P1**, **P2**, and **P3** are red-shifted by 44, 36, and 28 nm, respectively. This is due to the intramolecular electron transfer between the electron donor and electron acceptor units, which leads to the red-shifted absorption λ_{max}. The magnitude of spectral red-shift progressively decreases with the decrease in percentage of the electron acceptor (benzothiadiazole) in the polymers **P1–3**. The optical band gap was estimated according to the onset of absorption, showing that it gradually reduced from 2.38 eV for **P1** to 2.19 eV for **P3** with the decrease in percentage of the electron acceptor unit in the polymers (Table 2).

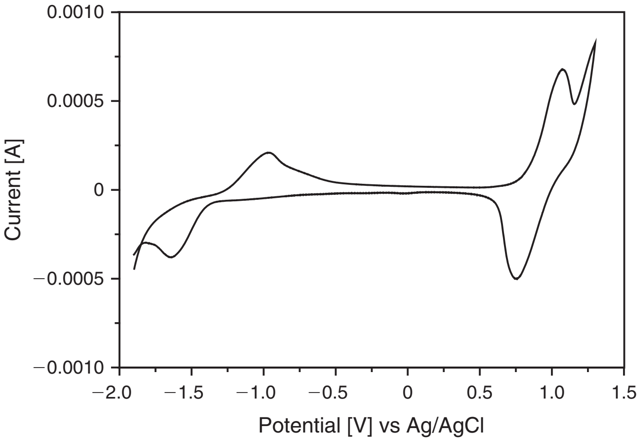

Fig. 4. Cyclic voltammogram of polymer **P3** on ITO coated PET in 0.1 M $LiClO_4$/ACN at a scan rate of 50 mV s^{-1}.

Table 3. Electrochemical properties of polymers P1 – P3

Polymer	Oxidation $E_{p,a}$ [V]^A	Reduction $E_{p,c}$ [V]^B	E_{ox} [V]^C	E_{red} [V]^C	I_p (HOMO) [eV]^D	E_a(LUMO)[eV]^D	E_g^{Ec} [eV]^E
P1	1.06	−1.65	0.99	−1.41	−5.39	−2.99	2.40
P2	1.03	−1.64	0.85	−1.44	−5.25	−2.96	2.29
P3	1.07	−1.64	0.85	−1.40	−5.25	−3.00	2.25

[A] Anodic oxidation peak potential.

[B] Cathodic reduction peak potential.

[C] E_{ox} and E_{red} are the onset potentials of oxidation and reduction respectively.

[D] I_p and E_a are the ionisation potential and electron affinity respectively; $I_p = -(E_{ox} + 4.4)$ eV, $E_a = -(E_{red} + 4.4)$ eV.[25]

[E] Electrochemical band gap = E_g^{Ec} = LUMO – HOMO.

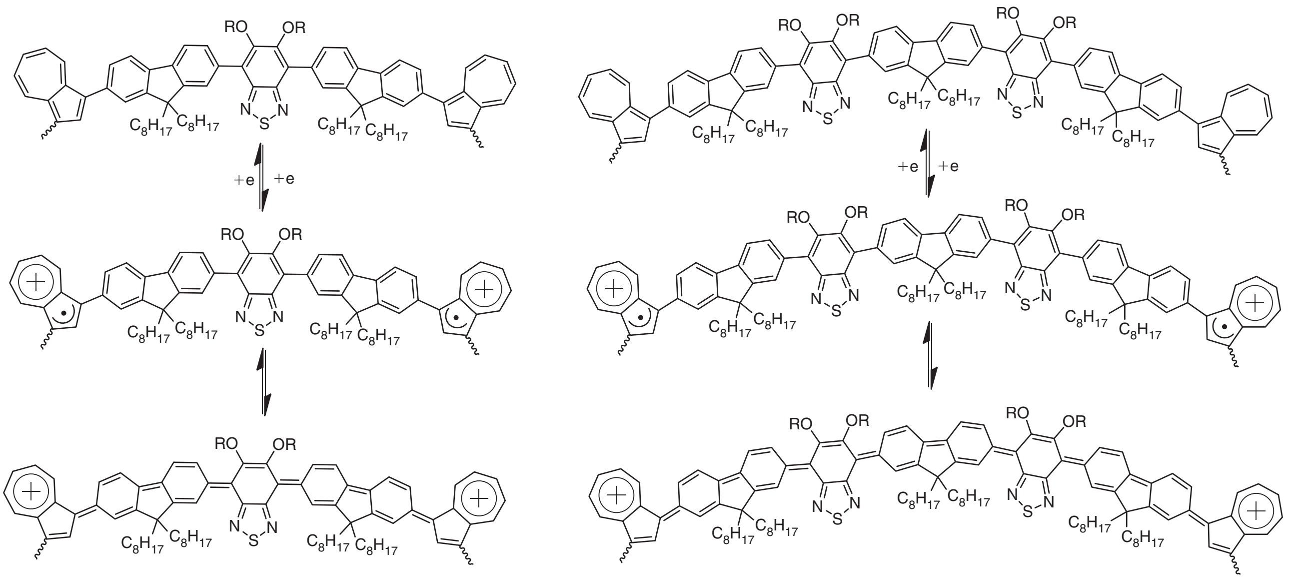

Scheme 2. Oxidation pathway of polymer **P2**

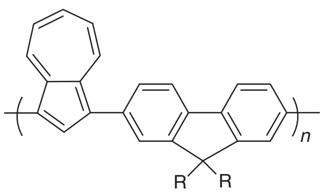

P4: R = $CH_2CH(C_2H_5)C_4H_9$

Chart 1.

The quantum yields, φ_{PL}, of polymers **P1–3**, were measured in dilute THF solutions using quinine sulfate (0.1 M in H_2SO_4) as a standard.[17] It was observed that the photoluminescence quantum yields of the polymers, φ_{PL} are significantly lower than other aromatic conjugated polymers. It was previously proposed that the incorporation of non-protonated azulene units in the polymer backbone could lead to a significant reduction in photoluminescence of the polymers as the non-protonated azulene units may act as quenchers to photoluminescence.[13b] This explanation supports the trend observed as the φ_{PL} decreases with the increase of azulene moieties from **P1** to **P3**. For instance, **P1** and **P2** with mole percentage of azulene of 30 and 50 %, respectively, are weakly fluorescent with a φ_{PL} of 0.013 and 0.0029; however, the polymer **P3** with mole percentage of 70 % azulene is completely non-emissive, which is similar to the polymer **P4**.

Electrochemical Behaviour of Polymers and Cyclic Voltammetry (CV)

Cyclic voltammetry measurements on spin-coated polymer films of **P1–3** were conducted in ACN with lithium perchlorate as the electrolyte and their CV data are summarised in Table 3. All potentials were measured against the Ag/Ag$^+$ reference couple. A typical cyclic voltammogram of polymer **P2** is illustrated in Fig. 4. The polymer **P2** showed one reversible oxidation redox wave in the range of 0.6–1.1 V under an anodic sweep. Being a random copolymer with two major repeating units, the probable oxidation pathway of the polymer **P2** is shown in Scheme 2. Azulene exists as an electron-rich five-membered ring fused to an electron-deficient seven-membered ring and thus the electron removal of the polymer **P2** usually occurs at the electron-rich cyclopentadiene part of the azulene ring to generate a cationic radical, which further rearranges to form a closed shell structure. The formation of similar tropylium cation radicals for azulene and its derivatives have been identified by electron spin resonance spectroscopy.[18]

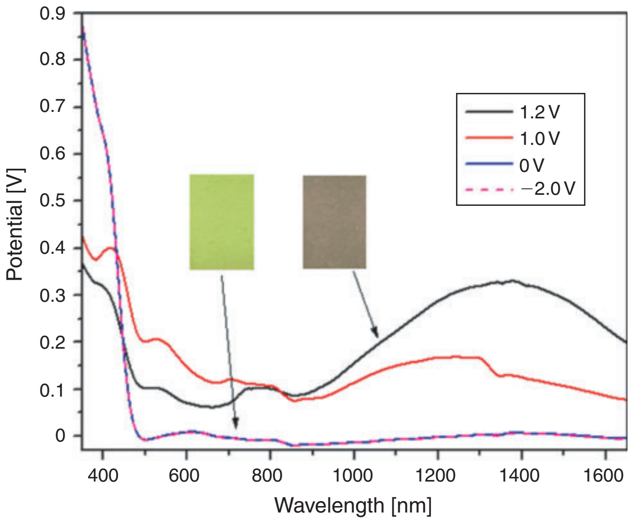

Fig. 5. Spectro-electrochemistry of polymer **P3** film on ITO coated PET in 0.1 M $LiClO_4$/ACN electrolyte/solvent couple.

The energy levels of the HOMO and LUMO of the polymers **P1–3** were estimated from the oxidation and reduction onsets in the cyclic voltammograms and the onset of absorption λ_{max} in the UV-Vis spectra, and the results are given in Table 3. Incorporation of azulene units into the conjugated polymers **P1–3** leads to a considerable decrease in oxidation of potentials. For example, polymer **P1** ($E_{p.a} = 1.06$ V vs Ag/AgCl) has a lower anodic oxidation peak potential (by 0.53 V) than homopolymer poly(9,9-dihexylfluorene) ($E_{p.a} = 1.59$ V[19] vs Ag/AgCl). Similarly, the electrochemical band gap values of the polymers **P1–3** (2.40–2.25 eV) are lower compared to homopolymer poly(9,9-dihexylfluorene) ($E_g = 2.86$ eV[19]). However, the band gaps of the polymers **P1–3** are higher than that of our reported polymers, for example, **P4** with a band gap of 1.6 eV. This is because the reported band gap of the reference polymer **P4** is calculated according to the onset of absorption of 630 nm, which belongs to the S_0-S_1 absorption band. The inclusion of the azulene unit in polymer **4** resulted in three bands at 630, 477, and 355 nm. In contrast, in this case, when an acceptor monomer dialkoxybenzothiadiazole is included in the polymer backbone, the band at around 600 nm disappeared. Therefore, the band gap is estimated in terms of the onset of the absorption band around 400 nm. If the onset of absorption of the most intense peak of the reference polymer **P4** ($\lambda_{max} = 355$ nm) is used for estimation of its band gap, the band gap of **P4** is around 2.85 eV, which is much higher than the band gap of the polymers **P1–3**. This reveals the ability of the acceptor units to lower the band gaps through domination of the LUMO level (Chart 1).

By varying the composition of azulene and benzothiadiazole in the polymers, the polymers **P1–3** showed slight differences for both oxidation and reduction peak potentials. The HOMO and LUMO levels of **P1–3** are calculated in terms of the onset of their oxidation and reduction waves. The electrochemical band gaps of 2.40, 2.29, and 2.25 eV, for **P1**, **P2**, and **P3** respectively, are slightly larger than that of corresponding optical band gaps deduced from the absorption spectra (2.38, 2.27, and 2.19 eV).

In addition, both optical band gaps and electrochemical band gaps increase with an increase in acceptor moieties from **P3** to **P1**. This is contrary to the expected results whereby an increase in mole percentage of acceptor moieties would result in a decrease in band gap. A possible explanation for the observations could be the significant increase in steric effects from the two alkyloxy side chains with the incorporation of more 5,6-bis(dodecyloxy)benzo-2,1,3-thiadiazole acceptor moieties. The steric effects imposed by two alkyloxy side chains considerably affects the co-planarity of the polymers which give rise to a shorter effective π-conjugation chain length and eventually a higher band gap as observed.[20] Another plausible reason is that co-monomer azulene plays a more important role in governing the band gap than the electron acceptor. Azulene is a non-alternate aromatic compound with peculiarly lower oxidation potential (+ 0.96 V vs SCE) than fused aromatic compounds such as naphthalene, and it is able to reduce the band gap when it acts as a co-monomer in conjugated polymers. Therefore, the higher the percentage of azulene in polymers is, the lower the band gap.

Spectro-Electrochemistry and Electrochromic Behaviour of Polymers

Spectro-electrochemical studies on the polymers were carried out in a 0.1 M $LiClO_4$/ACN electrolyte/solvent couple while increasing the applied potential from − 2 V to about + 1.6 V. Upon increasing applied potentials, the absorption at λ_{max} in the visible region is suppressed, with a concomitant formation of the absorption band in the near infrared (NIR) region. This is believed to be due to the formation of low-energy polarons and bipolarons. As a result, the colour of the polymers changed from yellowish green at 0 and − 2.0 V at the initial neutral state and electrochemically reduced state to greyish brown at the oxidised state as shown in Fig. 5. These changes are observed in all three polymers but the effect of the colour change is more pronounced in **P3**. Based on the onset of the π-π* transition, the spectro-electrochemical band gaps of **P1 – P3** are estimated and summarised in Table 3. The spectro-electrochemical band gaps are found to be in good agreement with the electrochemical band gaps. However, their values are slightly lower compared with those determined electrochemically. This difference is due to the interface barrier present between the polymer film and electrode, which results in a higher potential required during cyclic voltammetry for hole and charge injection.[18a] Hence, this gives rise to the higher values determined for the electrochemical band gaps.

Table 4. Optical contrast and switching speeds of polymers P1 – P3
NA: not applicable

Polymer	Optical contrast^A [%]		Switching speed^B [s]			
	UV-Vis^C	NIR^D	Coloration		Bleaching	
			UV-vis^C	NIR^D	UV-vis^C	NIR^D
P1	–	6	–	7.1	–	8
P2	4	17	3.8	7.0	9.4	4.8
P3	2	13	4.5	9.1	10.7	2.3
P4	NA	NA	8.1	NA	6.8	NA

^{A}Thin film of polymers were stepped between − 1.8 V and + 1.8 V using a square wave potential.

^{B}Switching speeds were calculated as the time required to obtain 95 % of full switch.

^{C}UV-Vis analysis performed at 410, 396, and 386 nm for **P1**, **P2**, and **P3** respectively.

^{D}NIR analysis performed at 1265, 1325, and 1365 nm for **P1**, **P2**, and **P3** respectively.

To probe the electrochromic properties of the polymers, a square-wave potential step absorptiometry was utilised. The polymer thin films were stepped between their oxidised (1.8 V) and reduced states (−1.8 V) at 10 s intervals. The percent transmittance changes were monitored as a function of time at λ_{max} and NIR region. The optical contrasts achieved for the polymers are summarised in Table 4. It can be seen that the electrochromic contrasts obtained at the NIR region are higher as compared with those obtained at λ_{max} in the visible regions. In particular, **P2** and **P3** show electrochromic contrasts of 17 and 13 % respectively at the NIR region (Fig. 6). Introduction of an electron acceptor moiety into the azulene copolymer improved the redox stability and thus more cycles were observed, but the gradual drop in the optical contrasts of the polymers upon repeated cycling reveals that the stability of such polymers needs further improvement. This is probably due to the two electron-donating alkoxy substituents in the benzothiadiazole, which weaken the overall electron-accepting ability of this electron acceptor and hence lead to limited improvement. The switching speeds of the polymers are calculated as the time required to obtain 95 % of the full optical contrasts. It is observed that the coloration speeds for **P1 – P3** measured at both UV-Vis and NIR wavelengths are slower than those of the azulene-fluorene copolymer. The bleaching speeds of **P2** and **P3**, on the other hand, are significantly faster compared with their coloration speeds. The incorporation of small and moderate amounts of acceptor units in **P3** and **P2** respectively helps to improve the bleaching speeds of the polymer. Among the three polymers, **P3** displays better switching speeds with a coloration time of 4.5 s and a bleaching time of 2.3 s at the visible and NIR wavelengths, respectively.

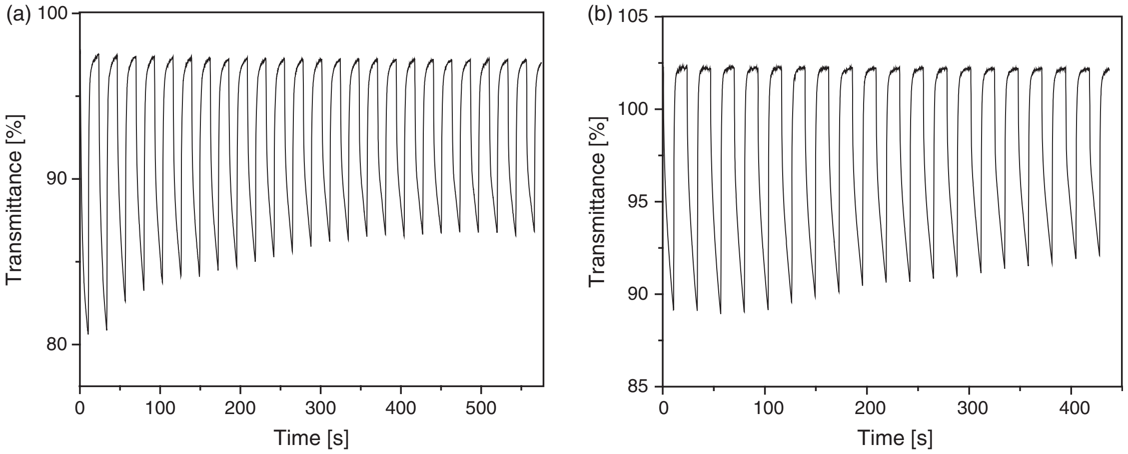

Fig. 6. Square-wave potential step absorptiometry of (a) polymer **P2** and (b) polymer **P3** films at 1325 nm and 1365 nm respectively on an ITO coated PET in 0.1 M $LiClO_4$/ACN electrolyte/solvent couple between − 1.8 V and + 1.8V with a switch time of 10 s.

Conclusions

A series of random π-conjugated copolymers were synthesised from 1,3-dibromoazulene, 4,7-dibromo-5,6-bis(dodecyloxy) benzo-2,1,3-thiadiazole, and 9,9-dioctylfluorene-2,7-bis (trimethyleneborate) via Suzuki cross-coupling reactions. The effect of electron acceptor and azulene units on the optical and electrochemical properties was studied. Polymers showed red-shifted absorption λ_{max} when compared with the reference polymer poly(azulene-*alt*-dioctylfluorene). Polymers **P1** and **P2** are fluorescent with low quantum yields of 0.013 and 0.0029, respectively, but, **P3** is non-fluorescent due to its high azulene content. The optical band gaps are in good agreement with the electrochemical band gaps. Subsequent electrochromic studies revealed that incorporation of an electron acceptor into azulene-containing conjugated polymers to some extent enhanced redox stability. These polymers displayed a colour change from yellowish green to greyish brown upon oxidation, with optical contrasts of 17 and 13 % in the NIR region.

Supplementary Material

The ^1H NMR spectra of polymers **P1** and **P3** and the elemental analysis data of polymers **P1**–**3** are available on the Journal's website.

Acknowledgement

We thank the Institute of Materials Research and Engineering (IMRE), Agency for Science, Technology and Research (A*STAR) for financial support.

References

[1] A. C. Grimsdale, K. L. Chan, R. E. Martin, P. G. Jokisz, A. B. Holmes, *Chem. Rev.* **2009**, *109*, 897. doi:10.1021/CR000013V

[2] A. C. Arias, J. D. MacKenzie, I. McCulloch, J. Rivnay, A. Salleo, *Chem. Rev.* **2010**, *110*, 3. doi:10.1021/CR900150B

[3] Y. J. Cheng, S. H. Yang, C. S. Hsu, *Chem. Rev.* **2009**, *109*, 5868. doi:10.1021/CR900182S

[4] A. A. Argun, P. H. Aubert, B. C. Thompson, I. Schwendeman, C. L. Gaupp, J. Hwang, N. J. Pinto, D. B. Tanner, A. G. MacDiarmid, J. R. Reynolds, *Chem. Mater.* **2004**, *16*, 4401. doi:10.1021/CM049669L

[5] P. M. Beaujuge, J. R. Reynolds, *Chem. Rev.* **2010**, *110*, 268. doi:10.1021/CR900129A

[6] S. K. Deb, *Appl. Opt.* **1969**, *8*, 192.

[7] R. M. Paul Monk, D. Rosseinsky, *Electrochromism and Electrochromic Devices* **2007** (Cambridge University Press: Cambridge).

[8] P. M. Beaujuge, S. Ellinger, J. R. Reynolds, *Nat. Mater.* **2008**, *7*, 795. doi:10.1038/NMAT2272

[9] (a) C. M. Amb, A. L. Dyer, J. R. Reynolds, *Chem. Mater.* **2011**, *23*, 397. doi:10.1021/CM1021245
(b) P. Shi, C. M. Amb, E. P. Knott, E. J. Thompson, D. Y. Liu, J. Mei, A. L. Dyer, J. R. Reynolds, *Adv. Mater.* **2010**, *22*, 4949. doi:10.1002/ADMA.201002234
(c) A. L. Dyer, E. J. Thompson, J. R. Reynolds, *ACS Appl. Mater. Interfaces* **2011**, *3*, 1787. doi:10.1021/AM200040P

[10] (a) E. Bundgaard, F. C. Krebs, *Macromolecules* **2006**, *39*, 2823. doi:10.1021/MA052683E
(b) O. Atwani, C. Baristiran, A. Erden, G. Sonmez, *Synth. Met.* **2008**, *158*, 83. doi:10.1016/J.SYNTHMET.2007.12.013
(c) J. Subbiah, P. M. Beaujuge, K. R. Choudhury, S. Ellinger, J. R. Reynolds, F. So, *ACS Appl. Mater. Interfaces* **2009**, *1*, 1154. doi:10.1021/AM900116P
(d) T. L. Wang, A. C. Yeh, C. H. Yang, Y. T. Shieh, W. J. Chen, T. H. Ho, *Sol. Energy Mater. Sol. Cells* **2011**, *95*, 3295. doi:10.1016/J.SOLMAT.2011.07.021

[11] F. Wang, Y. H. Lai, *Macromolecules* **2003**, *36*, 536. doi:10.1021/MA025662I

[12] L. Jönsson, *Acta Chem. Scand. A* **1981**, *35b*, 683. doi:10.3891/ACTA.CHEM.SCAND.35B-0683

[13] (a) W. C. Neikam, M. M. Desmond, *J. Am. Chem. Soc.* **1964**, *86*, 4811. doi:10.1021/JA01076A017
(b) R. J. Waltman, J. Bargon, *Can. J. Chem.* **1986**, *64*, 76. doi:10.1139/V86-015

[14] (a) G. Tourillon, F. Garnier, *J. Electroanal. Chem.* **1982**, *135*, 173. doi:10.1016/0022-0728(82)90015-8
(b) M. Iyoda, K. Sato, M. Oda, *Tetrahedron Lett.* **1985**, *26*, 3829. doi:10.1016/S0040-4039(00)89262-X
(c) R. J. Waltman, J. Bargon, *Can. J. Chem.* **1986**, *64*, 76. doi:10.1139/V86-015
(d) K. G. Neoh, E. T. Kang, T. C. Tang, *Polym. Bull.* **1988**, *19*, 325. doi:10.1007/BF00263932
(e) J. Daub, M. Feuerer, A. Mirlach, J. Salbeck, *Synth. Met.* **1991**, *42*, 1551. doi:10.1016/0379-6779(91)91897-J
(f) W. Schuhmann, J. Huber, A. Mirlach, J. Daub, *Adv. Mater.* **1993**, *5*, 124. doi:10.1002/ADMA.19930050211
(g) M. Porsch, G. Sigl-Seifert, J. Daub, *Adv. Mater.* **1997**, *9*, 635. doi:10.1002/ADMA.19970090809
(h) F. X. Redl, O. Köthe, K. Röckl, W. Bauer, J. Daub, *Macromol. Chem. Phys.* **2000**, *201*, 2091. doi:10.1002/1521-3935(20001001)201:15<2091::AID-MACP2091>3.0.CO;2-4
(i) F. Wang, Y. H. Lai, N. M. Kocherginsky, Y. Y. Koteski, *Org. Lett.* **2003**, *5*, 995. doi:10.1021/OL0274615

(j) B. Meana-Esteban, C. Lete, C. Kvarnstroem, A. Ivaska, *J. Phys. Chem. B* **2006**, *110*, 23343. doi:10.1021/JP063181L

(k) G. Nie, T. Cai, S. Zhang, J. Hou, J. Xu, X. Han, *Mater. Lett.* **2007**, *61*, 3079. doi:10.1016/J.MATLET.2006.11.004

[15] (a) S. E. Estdale, R. Brettle, D. A. Dummur, C. M. Marson, *J. Mater. Chem.* **1997**, *7*, 391. doi:10.1039/A606139G

(b) F. Wang, Y. H. Lai, *Macromolecules* **2003**, *36*, 536. doi:10.1021/MA025662I

(c) F. Wang, Y. H. Lai, M. Han, *Org. Lett.* **2003**, *5*, 4791. doi:10.1021/OL0357346

(d) Z. Hussain, H. Hopf, L. Pohl, T. Oeser, A. K. Fischer, P. G. Jones, *Eur. J. Org. Chem.* **2006**, 5555. doi:10.1002/EJOC.200500733

(e) X. Wang, J. K. Ng, P. Jia, T. Lin, C. M. Cho, J. Xu, X. Lu, C. He, *Macromolecules* **2009**, *42*, 5534. doi:10.1021/MA900847R

(f) M. Murai, E. Amir, R. J. Amir, C. J. Hawker, *Chem. Sci.* **2012**, *3*, 2721. doi:10.1039/C2SC20615C

[16] J. Bouffard, T. M. Swager, *Macromolecules* **2008**, *41*, 5559. doi:10.1021/MA8010679

[17] A. N. Fletcher, *Photochem. Photobiol.* **1969**, *9*, 439. doi:10.1111/J.1751-1097.1969.TB07311.X

[18] (a) C. J. Cooksey, J. L. Courtneidge, A. G. Davies, P. S. Gregory, J. C. Evans, C. C. Rowlands, *J. Chem. Soc., Perkin Trans. 2* **1988**, 807. doi:10.1039/P29880000807

(b) F. Gerson, M. Scholz, H. J. Hansen, P. Uebelhart, *J. Chem. Soc., Perkin Trans. 2* **1995**, 215. doi:10.1039/P29950000215

[19] B. Liu, W. L. Yu, Y. H. Lai, W. Huang, *Chem. Mater.* **2001**, *13*, 1984. doi:10.1021/CM0007048

[20] H. Yi, S. Al-Faifi, A. Iraqi, D. C. Watters, J. Kingsley, D. G. Lidzey, *J. Mater. Chem.* **2011**, *21*, 13649. doi:10.1039/C1JM12089A